

## Limits of ultrashort pulse generation in cw mode-locked dye lasers

V. Petrov, W. Rudolph, U. Stamm, and B. Wilhelmi

*Department of Physics, Friedrich-Schiller-University, DDR-6900 Jena, German Democratic Republic*

(Received 15 September 1988; revised manuscript received 6 March 1989)

Essential mechanisms limiting the achievable pulse duration in synchronously pumped, hybrid-mode-locked, and passively mode-locked cw subpicosecond dye lasers are analyzed. The action of spontaneously emitted light is shown to be the detrimental factor in synchronous mode locking. The influence of this factor can be suppressed by a saturable absorber in the hybrid-mode-locked lasers. In this case as well as in the case of passive mode locking the combined action of group-velocity dispersion and Kerr-effect-type nonlinearity, though serving as an additional shortening mechanism, causes fluctuations of the pulse parameters and determines the limit of the steady-state regime.

### I. INTRODUCTION

Because of their large amplification, bandwidth dye lasers can advantageously be used to generate light pulses of subpicosecond duration.<sup>1</sup> For the study of very fast phenomena, the periodic trains of pulses generated by cw lasers are very attractive since powerful signal averaging and processing techniques are available. Various methods for pulse generation have been developed to satisfy different requirements for the pulse parameters. Synchronous mode locking provides tunable pulses of picosecond duration, but requires a mode-locked pump source [Ar<sup>+</sup> or second-harmonic neodymium-doped yttrium aluminum garnet (Nd:YAG) laser]. Passive mode locking is relatively simpler to realize since it requires only a cw pumping. For a long time the shortest pulses directly generated in lasers (27 fs) have been achieved by this method.<sup>2</sup> The wavelength tunability, however, is lost. A technique which combines some of the advantages of the above two, i.e., femtosecond pulses and higher-output energies, is hybrid mode locking. The synchronism between the pump laser and the femtosecond pulse train is advantageous here with respect to subsequent synchronous amplification. Recently, hybrid mode locking was shown to be able to produce pulses shorter than 30 fs also.<sup>3</sup> The considerable progress in all these techniques during the last decade is mainly due to improvements of the cavity design and all cavity elements. The continuous reduction of the pulse duration revealed that a great number of effects are responsible for the maximum shortening that can be achieved, as well as for the steady-state regime established in such lasers. The latter cannot be regarded simply as a result of the combined action of an active medium and a mode locker. Analytical treatment previously developed<sup>4-6</sup> is at present unable to account for the complexity of these systems. Recently, numerical models based on ring schemes of the resonators were used to describe synchronous<sup>7-9</sup> as well as passive mode locking.<sup>10,11</sup> These models require no preliminary assumptions concerning the shape of the steady-state solution and allow one, in addition, to

study transient evolution, as well as the influence of spontaneous emission or pump laser fluctuations on the mode-locking regime. We present here an analysis of the limitations of all three types of cw dye lasers. The basic features of the approaches<sup>10,12</sup> are preserved, while hybrid mode locking is regarded as an extension of synchronous mode locking by a saturable absorber. This approach enables the investigation of the influence of the cavity mismatch, which, however, is not so well pronounced as in the synchronous mode locking. Some of the results concerning passive mode locking can also be interpreted for hybrid mode locking under optimum synchronization conditions.

### II. ROUND TRIP MODEL AND BASIC EQUATIONS

A general scheme including all possible resonator elements is presented in Fig. 1. This ring model, as previous studies have shown,<sup>10,12</sup> can provide a realistic picture of the process engaged, though the effects of colliding pulse mode locking in ring cavities, as well as double passage through some elements in linear cavities, are not taken into account. A steady state for this system can be searched in the sense of a slowly varying complex amplitude of the electric field of the intracavity pulse  $\bar{E} = |\bar{E}| \exp(i\phi)$  which reproduces itself after one cavity round trip. Thus a basic approximation in the model is the representation of the electric field as a slowly varying envelope and a fast oscillating phase factor. Assuming further a linearly polarized electric field propagating along the  $z$  coordinate, we have

$$E(z, t) = \frac{1}{2} \bar{E}(z, t) \exp[i(\omega_L t - k_L z)] + \text{c.c.}, \quad (1)$$

where  $k_L = \omega_L / c$  is the wave number defined at  $\omega_L$ . The equation for one cavity transit can be written in coordinates moving with the pulse  $\xi = z$ ,  $\eta = t - z/v$ ,

$$\bar{E}'(\eta) = \bar{O} \{ \bar{E}(\eta) \}, \quad (2a)$$

where  $v$  is the pulse velocity and  $\bar{O}$  is the operator which

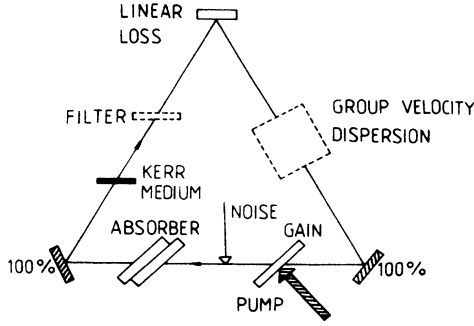


FIG. 1. Schematic of the resonator model.

describes the action of all cavity elements on the slowly varying complex amplitude of the laser pulse. The prime denotes the envelope after one cavity round trip.

In general, we will use an expression of the type of (2a) to calculate the formation of the laser pulses by the mode-locking techniques under consideration. A steady state is reached if the slowly varying envelope reproduces itself after one transit through the cavity:

$$\bar{E}'(\eta+h) = \bar{E}(\eta). \quad (2b)$$

Strictly speaking, an additional small constant phase shift per round trip can also be included in (2b). This phase shift would correspond to a modified phase velocity of the pulse. Since our numerical treatment is in the slowly varying envelope approximation, this phase shift has no physical meaning. The velocity  $v$  can be assumed to be equal to the phase velocity in the absence of dispersion, or to the group velocity if dispersion is considered, and, accordingly, is determined by the linear optical properties of each cavity element. In any case, the small local time shift  $h$  represents a deviation of the resonator round trip time calculated for  $v$  from the actual transit time determined by the velocity of the pulse envelope. The latter is determined by the linear and nonlinear processes involved. In synchronous or hybrid mode locking this deviation corresponds to the mismatch of the cavity lengths of the pump and dye lasers, whereas for passive mode locking it results from the difference of group and envelope velocity in each cavity element.

In general, the steady-state condition (2b) can be applied at different positions in the scheme of Fig. 1. For synchronous as well as hybrid mode locking, this would result in differing solutions. Without loss of generality, however, a definite position can be assumed (e.g., after the outcoupling mirror) in order to study the essential dependencies of the pulses on the parameters characterizing the resonator elements. The situation in passive mode locking is additionally simplified, since all cavity elements modify only slightly the complex field envelope and, within first-order terms, all positions in Fig. 1 are interchangeable.

The interaction of the propagating pulse with the near-resonant molecules of the gain and of the absorber media can be described by the combined system of density matrix and wave equations. The molecules can be

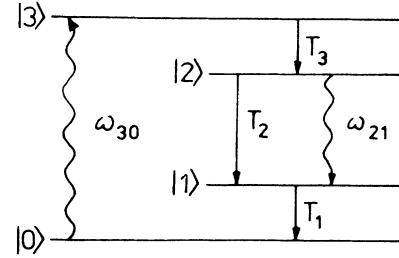


FIG. 2. Four-level scheme modeling a dye molecule.

represented by an effective four-level system (Fig. 2), where  $|0\rangle \rightarrow |3\rangle$  is the transition interacting with the pump radiation and  $|2\rangle \rightarrow |1\rangle$  is the lasing transition in the case of gain medium. In the case of a saturable absorber the intracavity pulse interacts with the  $|0\rangle \rightarrow |3\rangle$  transition. Only homogeneous broadening will be considered in this system. For the vibrational relaxation times  $T_1$  and  $T_3$ , for the singlet lifetime  $T_2$  as well as for the phase (polarization) relaxation times, different approximations will be applied according to the time scale considered.

### III. SYNCHRONOUS MODE LOCKING

In the ring model in Fig. 1 we take into account the active dye, the nonsaturable loss, and the filter element. The picosecond duration of the pump laser pulses justifies here the assumption of fast thermalization in the S0 and S1 bands ( $T_1, T_3 \ll T$ ). Thus the system in Fig. 2 becomes effectively a three-level system for the gain medium.

The bandwidth-limiting element shall be described by a Lorentzian line-shape function  $\mathcal{L}_F$  the center of which equals the laser frequency  $\omega_L$ . Thus we have

$$\mathcal{L}_F(\omega - \omega_L) = [1 + i\tau_F(\omega - \omega_L)]^{-1}, \quad (3)$$

where  $\tau_F$  is the characteristic response time of such a filter. The spectral width of the intracavity filter element should be smaller than the bandwidth of the amplifying dye in order that the rate equation approximation (REA)—the phase relaxation time is assumed to be much shorter than the pulse duration  $T$ —can be applied.

With these assumptions the amplification of the slowly varying complex envelope of the electric field of the intracavity pulse is given by

$$\bar{E}^{\text{out}}(\eta) = G^{1/2}(\eta)\bar{E}^{\text{in}}(\eta) + \tilde{E}(\eta), \quad (4)$$

where  $|G(\eta)|$  is the time-dependent intensity gain and  $\tilde{E}(\eta)$  accounts for spontaneously emitted light. The gain  $G(\eta)$  is determined by  $G(\eta) = \exp[g(\eta)/\mathcal{L}_a]$ , where  $g(\eta)$  satisfies the ordinary differential equation

$$\frac{dg(\eta)}{d(\eta/2\tau_F)} = F_p(\eta) - F(\eta)\{\exp[g(\eta)] - 1\} - 2\tau_F g(\eta)/T \quad (5)$$

In the above expression for  $G(\eta)$ ,  $\mathcal{L}_a$  is the line-shape

function for the laser transition  $|2\rangle \rightarrow |1\rangle$  and reads

$$\mathcal{L}_a = [1 + i\tau_a(\omega - \omega_a)]^{-1}, \quad (6)$$

where  $\tau_a$  is the corresponding phase relaxation time and  $\omega_a$  is the transition frequency. In what follows, the subscript  $a$  is used for quantities related to the  $|2\rangle \rightarrow |1\rangle$  transition of the gain medium,  $\text{Re}$  will denote the real part, and the asterisk the conjugate complex of a quantity. For convenience we normalize the time coordinate by the filter response time  $\tau_F$  and use normalized (dimensionless) intensities of the laser and pump pulse in (5), i.e.,  $F(\eta) = \tau_F \sigma_a k_L |\bar{E}|^2 / \hbar \mu_0 \omega_L$  and  $F_p(\eta) = \tau_F \sigma_a k_p |\bar{E}_p|^2 / \hbar \mu_0 \omega_p$ .  $\bar{E}_p$  is the slowly varying envelope of the electric field of the pump pulse and  $\omega_p$  is its carrier frequency, which is assumed to be in resonance with the transition  $|0\rangle \rightarrow |3\rangle$ .

For the pump pulse a Gaussian shape is assumed:

$$F_p(\eta) = (2/\sqrt{\pi}) \epsilon_p s \text{Re}(\mathcal{L}_a)(\tau_F/T_p) \exp[-(\eta/T_p)^2]. \quad (7)$$

$\epsilon_p$  is the energy, normalized to the saturation energy of the pump transition,  $T_p$  the duration of the pump pulse,  $\sigma_{03}$  the absorption cross section, and  $s = \sigma_a / \sigma_{03}$  the ratio of the cross sections in the centers of the lines.

On the right-hand side of (4) we have added a time-dependent quantity  $\bar{E}(\eta)$  to take into account spontaneous emission. Originally, one has to introduce the corresponding fluctuation operator into the density matrix equations. In the special case considered here, however, the contribution of spontaneous emission to the laser field is very small during one cavity round trip and a phenomenological treatment is justified. In addition, we can neglect the saturation of the gain by spontaneous radiation in (5) for typical experimental conditions. Following Ref. 12 we assume the amplitude of the spontaneously emitted field to be Rayleigh-distributed and the phases to be equally distributed. Then the probability density is given by

$$\Pi(\bar{E}) = (\pi \langle |\bar{E}|^2 \rangle)^{-1} \exp(-|\bar{E}|^2 / \langle |\bar{E}|^2 \rangle), \quad (8)$$

with the ensemble average

$$\langle |\bar{E}(\eta)|^2 \rangle = A (4\hbar \mu_0 \omega_L^2 / \tau_F \sigma_a k_L) g(\eta). \quad (9)$$

The numerical factor  $A$  describes the magnitude of spontaneous emission. It can be estimated from

$$A = \frac{\tau_a \tau_F}{\pi} \int_{\omega_a - 1/\tau_F}^{\omega_a + 1/\tau_F} d\omega \int_{\Delta\Omega} d\Omega A_a |\mathcal{L}_a(\omega - \omega_a)|^2 G(\Omega),$$

with  $G(\Omega)$  as the angular distribution of spontaneous emission,  $A_a$  is the total fluorescence transition probability, and  $\Delta\Omega$  is the spatial angle of interest. For our calculation we estimate  $A \approx 10^{-10}$ . A complete cavity round trip of the laser pulse includes transits through the active dye, through the bandwidth limiting element, and through an intensity outcoupler with the outcoupling coefficient  $\gamma$ . Moreover, we have to take into account a shift  $h$  of the laser pulse in local time due to the different optical lengths of pump and dye laser. The cavity transit equation for the  $i$ th transit therefore reads

$$\begin{aligned} \bar{E}^{(i+1)}(\eta+h) = & \sqrt{1-\gamma} \int_{-\infty}^{\eta} \exp[-(\eta-\eta')/\tau_F] \\ & \times \{ G^{1/2}(\eta') \bar{E}^{(i)}(\eta') \\ & + \tilde{E}(\eta') \} d(\eta'/\tau_F). \quad (10) \end{aligned}$$

To determine the complex amplitude of the dye laser pulse, (10) is iterated starting with an input amplitude for the first cavity transit, which is determined from spontaneous emission corresponding to (8) and (9). A steady state is defined by (2b), which reads, with the present notation,

$$\bar{E}^{(i+1)}(\eta) = \bar{E}^{(i)}(\eta). \quad (11)$$

Due to the fluctuating character of spontaneous emission,

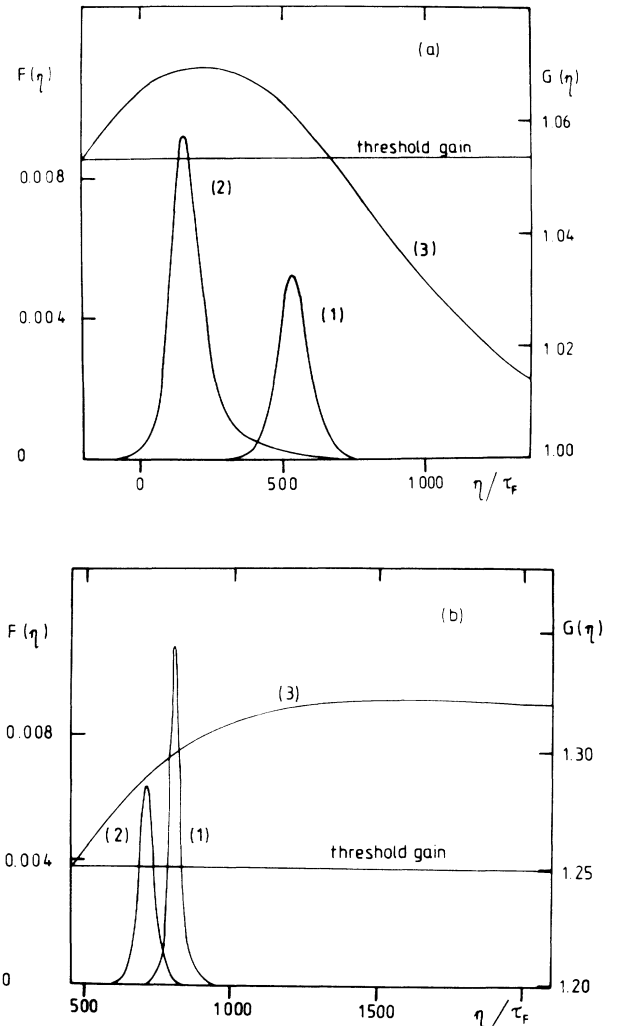


FIG. 3. Normalized pulse intensity for a fast [ $T_p/T_a = 3$ , (a)] and slowly [ $T_p/T_a = 0.01$ , (b)] relaxing gain without (1) and with (2) consideration of spontaneous emission. Parameters:  $A = 10^{-10}$ ,  $T_p/\tau_F = 800$ ,  $\tau_a(\omega_L - \omega_a) = 0$ ,  $h/\tau_F = 0$ , and  $s = 0.7$ . In the case of a fast dye  $\gamma = 0.05$  and  $\epsilon_p = 1.61$ , and in the case of a slow dye  $\gamma = 0.2$  and  $\epsilon_p = 1.18$ . The gain  $|G(\eta)|$  is also plotted (3).

(11) cannot be satisfied in an exact sense. In the following we apply (11) only around the pulse maximum and define the steady state as the reproduction of the pulse intensity better than 0.1%.

We proceed with the analysis of the influence of the contribution of the spontaneous emission in synchronously pumped dye lasers. In Fig. 3 the stationary normalized pulse intensities, with and without consideration of spontaneous emission, are shown for slowly [ $T_a \gg T_p$ , Fig. 3(a)] and fast [ $T_a < T_p$ , Fig. 3(b)] relaxing amplifying dyes. In both cases spontaneous emission results in a shift of the pulse to earlier times on the retarded-time axis. This is caused by the reconstruction of the pulse edges by spontaneous radiation (as discussed in Refs. 9 and 13). Since the laser is above threshold before the pulse passes through the gain medium, spontaneously emitted light at the leading edge is amplified from round trip to round trip. Thus in the presence of spontaneous emission an additional timing mismatch  $h_{sp}$  occurs. In the steady state the total timing mismatch equal to  $h + h_a + h_f + h_{sp}$  has to vanish ( $h_a$  and  $h_f$  represent time shift due to the action of the amplifier and filter, respectively). Thus spontaneous emission modifies the range of the geometrical (cavity) mismatch  $h$  in which single pulses are generated. For the example given in Fig. 3, the quantity  $h_{sp}$  is negative. It can be positive if the net gain  $|\bar{G}(\eta)|$  at the leading edge of the pulse is less than 1 (this means for larger negative cavity mismatch  $h$ ).

As a consequence pulse shape and peak intensity essentially differ with and without consideration of spontaneously emitted light, and it depends on the time behavior of the gain how strong the influence is. For the fast relaxing dye, for example, the peak intensity with spontaneous emission increases, whereas for the longer living dye the opposite behavior occurs.

The injection of spontaneously emitted light during each cavity transit of the laser pulse results in a background noise of the pulse.<sup>9,12</sup> Dependent on the operation conditions of the laser this may prevent a steady state even if it is defined as explained above. Especially the cavity length mismatch  $h$  has a pronounced effect on the laser stability. In general, the envelope of the pulses generated in synchronously pumped dye lasers is not smooth, but exhibits a substructure. In Fig. 4 the normalized pulse intensity is plotted for different cavity length mismatch. Obviously, pulses with substructure are generated for cavity mismatch  $h/\tau_F = -1.25$  and  $h/\tau_F + 1.25$  caused by the spontaneous emission. Only for  $h/\tau_F < 1$ , smooth single pulses reproducing themselves from round trip to round trip can be obtained. Note at higher pump intensity and larger intracavity filter bandwidth for  $h \approx 0$ , multiple pulses are generated around zero mismatch as well.<sup>12</sup> Neglecting spontaneous emission, an increase in the timing mismatch seems to allow the generation of short, smooth single pulses.<sup>4,7</sup> In practice, spontaneous emission leads to a considerable pulse broadening and causes instabilities in the formation process resulting in a structured pulse shape and lack of a steady state. Especially, one has to note that without intracavity bandwidth limitation the steady state cannot be reached, in contrast to the predictions in Ref. 14, since the reconstruction of the pulse

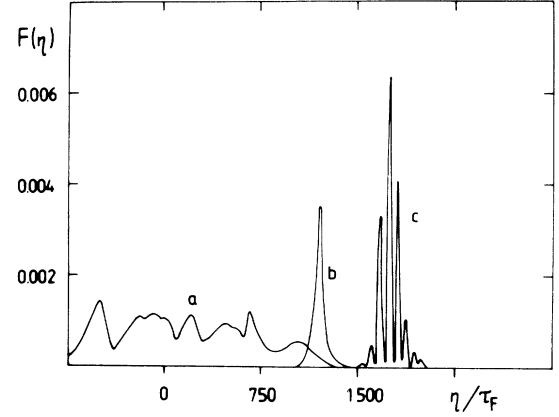


FIG. 4. Normalized pulse intensity in the case of synchronous mode locking for different cavity length mismatch (a)  $h/\tau_F = -1.25$ , (b)  $h/\tau_F = 0$ , and (c)  $h/\tau_F = 1.25$ . The other parameters are  $A = 10^{-10}$ ,  $\gamma = 0.2$ ,  $T_p/\tau_F = 1250$ ,  $\epsilon_p = 0.42$ ,  $\tau_a(\omega_L - \omega_a) = -0.75$ , and  $s = 1$ .

edges causes fluctuations which are not damped by the system. Thus the essential limitation to the pulse duration in synchronous pumping lies in the action of spontaneous emission, which limits the possible pump intensity and possible intracavity filter bandwidth in order to reach the steady state.

#### IV. HYBRID MODE LOCKING

In addition to the configuration discussed in the previous section, we include here a saturable absorber in the resonator model, see Fig. 1. The saturable absorber interacts only with the laser pulse and in a good approximation we have  $T_1 \ll T \ll T_2$ . Thus the absorber molecules can be modelled effectively by an ensemble of three-level systems<sup>1</sup> (see Fig. 2), the corresponding quantities of which are labelled by  $b$ . For the time-dependent absorption  $K(\eta)$ , an equation analogous to (5), but with  $Fp = 0$ , holds, which can be integrated to yield<sup>15</sup>

$$K^{\mathcal{L}_b^*}(\eta) = \exp[m_b \epsilon_a(\eta)] / \{ \exp[\kappa \text{Re}(\mathcal{L}_b)] - 1 + \exp[m_b \epsilon_a(\eta)] \}, \quad (12)$$

where  $\mathcal{L}_b$  is the corresponding line-shape function defined analogous to (6),

$$\epsilon_a(\eta) = \int_{-\infty}^{\eta} F(\eta') d(\eta'/2\tau_F)$$

is the time-dependent energy, normalized to the saturation energy of the  $|2\rangle \rightarrow |1\rangle$  transition of the gain medium, and  $m_b = m_b^0 \text{Re}(\mathcal{L}_b) / \text{Re}(\mathcal{L}_a) = q \sigma_b \text{Re}(\mathcal{L}_b) / [\sigma_a \text{Re}(\mathcal{L}_a)]$ , with  $q$  as factor describing different focusing in the absorber and gain medium.  $\kappa = \sigma_b \gamma_b L_b$  is the small signal absorption coefficient defined as the product of the cross section  $\sigma_b$ , the particle number density  $\gamma_b$ , and the thickness of the absorber jet  $L_b$ . Now the round trip equation takes the form

$$\begin{aligned} \bar{E}^{(i+1)}(\eta+h) = & \sqrt{1-\gamma} \int_{-\infty}^{\eta} \exp[-(\eta-\eta')/\tau_F] K^{1/2}(\eta') \\ & \times [G^{1/2}(\eta') \bar{E}^{(i)}(\eta') \\ & + \bar{E}(\eta')] d(\eta'/\tau_F). \end{aligned} \quad (13)$$

As expressed by (13), the saturable absorption leads to the suppression of spontaneously emitted light in front of the propagating pulse, whereas at the trailing pulse edge this does not happen when the absorber exhibits slow recovery. Nevertheless, due to gain saturation at the trailing edge of the pulse, spontaneously emitted light is also rapidly diminished. In this manner the hybrid-mode-locked laser is much less sensitive to the action of spontaneous emission than the synchronously pumped laser.

For illustration we consider the cavity mismatch behavior of the hybrid-mode-locked laser, see Fig. 5. The parameters are chosen in such a way that a direct comparison with Fig. 4 is possible. In particular, the losses have equal magnitude, but now they consist of two equal parts—a saturable and a nonsaturable contribution. As can be seen from Fig. 5 and Fig. 4, hybrid mode locking provides shorter pulse duration and increased peak intensity. In addition, the region of stable steady-state solutions covers a much broader cavity mismatch range. This is a result of the stabilization of the pulse velocity by the simultaneous action of gain and absorption. The absorber introduces an additional timing mismatch  $h_b$  which partially compensates the pulse advancing influence of the gain and spontaneous emission. Consequently, as opposed to synchronous mode locking, the timing mismatch for single pulse generation through hybrid mode locking remains around  $h/\tau_F < 1$ , even if the pump intensity is increased.

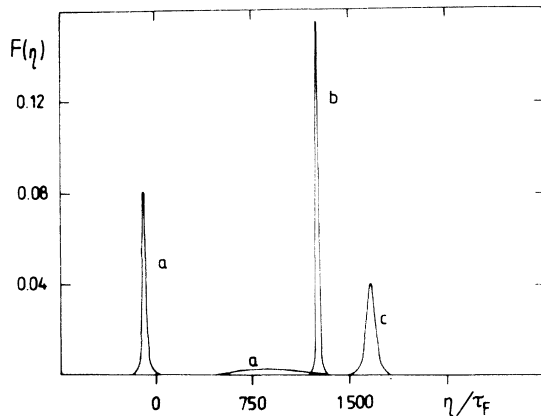


FIG. 5. Normalized pulse intensity in the case of hybrid mode locking for different cavity length mismatch (a)  $h/\tau_F = -1.25$ , (b)  $h/\tau_F = 0$ , and (c)  $h/\tau_F = 1.25$ . The other parameters are  $A = 10^{-10}$ ,  $\gamma = 0.1$ ,  $T_p/\tau_F = 1250$ ,  $\epsilon_F = 0.42$ ,  $\tau_a(\omega_L - \omega_a) = -0.75$ ,  $s = 1$ ,  $\kappa = 0.1$ ,  $\tau_b(\omega_L - \omega_b) = -1$ , and  $m_b^0 = 7.68$ .

In the above discussion we have omitted the frequency chirp of the laser pulse, though a phase modulation, due to the saturation of gain and absorption, is included in the equations. This phase modulation has an essential influence for laser pulses with several hundreds of femtoseconds pulse width. On this time scale the REA becomes invalid and the assumption of an additional bandwidth limiting element, with a width much smaller than the bandwidth of the saturable media, should be dropped. The particular influence that phase-modulating processes have on the pulse stability, is discussed in Sec. V in connection with passive mode locking.

## V. PASSIVE MODE LOCKING

The round-trip model includes all elements presented in Fig. 1, except the passive frequency filter. Such filter action in typical cavities is avoided in order to achieve ultimate short pulses. The only bandwidth-limiting effect arises then from the active dye and the saturable absorber through action of their finite transition profiles. Thus the REA cannot be applied, but instead the corresponding systems of density matrix equations have to be solved. Assuming homogeneously broadened transitions, this requires the consideration of a phase memory for the active media. The short pulse duration allows one to consider the case  $T \ll T_{1,3}$  which means that the system in Fig. 2 is effectively a two-level system.

The great number of effects [we note that a second (isomer) form of the saturable absorber should also be included<sup>16</sup>] considerably complicates the treatment of the steady-state equation. Though as mentioned above, and as it is experimentally proven, all elements shape the pulse only slightly and the corresponding transfer operators can be considered only up to first-order terms.

The Kerr-type nonlinearity and the dispersion have a decisive influence on the shaping of the phase of the pulse. While, for the dispersion effect, a lot of experimental evidence exists revealing its decisive role for the pulse shortening under 200 fs (see, e.g., Ref. 17) the influence of the nonlinearity is difficult to be measured independently of the other effects, and only recently experimental observations have been reported.<sup>18</sup>

We proceed with the analysis of instabilities appearing as a result of the interplay between dispersion and nonlinearity. We note that, in the presence of only saturable gain and absorption and nonsaturable loss, no such effects were observed in previous studies<sup>19</sup> if the laser is operated above threshold. The inclusion of dispersion and nonlinearity can result in shortening or lengthening of the pulse duration combined with phase modulation. The main question to be answered is whether it is possible to compress the pulse intracavity through the adjustment of dispersion and nonlinearity without onset of pulse deterioration or fluctuations of the pulse parameters. This compression would be useful only if it is more effective and leads to shorter pulses compared to extracavity compression of a similar pulse chirped inside the cavity.

We include the effects of group velocity dispersion and Kerr-effect-type nonlinearity in the numerical model

developed in Refs. 10 and 19. The resonant molecules are modeled by two-level systems and the phase memory is taken into account in the equation governing the polarization. This results in a transfer operator containing bandwidth-limiting properties which, however, are saturable.<sup>10</sup> If all energy terms are normalized to the saturation energy of the gain medium at the laser wavelength, the modification of the complex pulse envelope in the gain medium ( $a$ ) is

$$\delta_a \bar{E}(\eta) = \frac{g_a(1 - e^{-U/T_a})}{2\tau_a(1 - e^{-\varepsilon_a - U/T_a})} \times \int_{-\infty}^{\eta} d\eta' \bar{E}(\eta') \exp[(\eta' - \eta)/\mathcal{L}_a \tau_a - \varepsilon_a(\eta')] , \quad (14)$$

where  $g_a = \sigma_a \gamma_a L_a$  is the small signal gain at the leading edge of the pulse modified above to account for the fact that the round trip time  $U$  can be comparable with the energy-relaxation time of the gain  $T_a$  ( $T_2$ ), see Ref. 20,  $\mathcal{L}_a$  is defined from (6) for the  $|2\rangle \rightarrow |1\rangle$  transition and  $\tau_a$  is the corresponding phase-relaxation time. The normalized energy is

$$\varepsilon_a(\eta) = \beta_a \operatorname{Re} \mathcal{L}_a \left[ \int_{-\infty}^{\eta} d\eta' |\bar{E}(\eta')|^2 \right] , \quad (15)$$

where  $\beta_a = |\mu_m|^2 \tau_a / h^2$ , with  $\mu_m$  as the dipole moment.  $\varepsilon = \varepsilon_a(\infty)$  denotes the total energy and  $\varepsilon_{st}$  is the steady-state value of  $\varepsilon$ . Similarly, for the saturable absorber ( $b$ ) and its second (photoisomer) form ( $c$ ), we have for the envelope change, assuming  $T_2 \ll U$ :

$$\delta_{b,c} \bar{E}(\eta) = (g_{b,c} / 2\tau_{b,c}) \times \int_{-\infty}^{\eta} d\eta' \bar{E}(\eta') \exp[(\eta' - \eta) / \mathcal{L}_{b,c} \tau_{b,c} - m_{b,c} \varepsilon_a(\eta')] . \quad (16)$$

[ $m_{b,c} = m_{b,c}^0 \operatorname{Re} \mathcal{L}_m$  are New's stability (saturation) parameters,<sup>21</sup> where  $m_{b,c}^0 = q\sigma_{b,c} / \sigma_a$  are the ratios of the corresponding interaction cross sections multiplied by a focusing factor  $q$ ;  $g_b = -\kappa(1-p)$  and  $g_c = -\kappa p m_c^0 / m_b^0$ , where  $\kappa$  is an effective absorption coefficient, which coincides with the total absorption if the two isomers have equal absorption profiles, and  $p$  is the photoisomer percentage.] The photoisomerized part of DODCI (the most commonly used absorber) can be estimated using a simplified model of DODCI dynamics,<sup>16</sup> where the distribution of the two species in the jet is assumed to be isotropic and no transversal effects are considered. Neglecting the exchange of excited state molecules through the jet flow during one round trip, we obtain in the steady-state regime

$$p = \Phi_p [1 - \exp(-m_b \varepsilon)] / \{ \mathcal{W} + \Phi_p [1 - \exp(-m_b \varepsilon)] + \Phi_d [1 - \exp(-m_c \varepsilon)] \} , \quad (17)$$

where  $\Phi_p$  and  $\Phi_d$  are the quantum yields for isomerization from the excited ground-state form and for the decay

reaction, respectively. The normalized velocity parameter for the dye flow is  $W = V = U/L_g$  ( $V$  is the flow velocity and  $L_g$  is the diameter of the focal spot in the DODCI jet).

The contribution of a nonlinear index medium (e.g., intensity-dependent refractive index of the dye solvents) and of the linear dispersion elements (e.g., intracavity prisms) can be considered by expansion of the corresponding polarization terms in the nonresonant wave equation.<sup>22</sup> Neglecting higher-order terms (nonlinear Schrödinger equation), we have for the pulse shaping in the nonlinear refractive index element

$$\delta_e \bar{E}(\eta) = -in_e \tau_a \beta_a \mathcal{L}_a |\bar{E}(\eta)|^2 \bar{E}(\eta) , \quad (18)$$

and in the group-velocity dispersion element,

$$\delta_d \bar{E}(\eta) = i(r\tau_a^2/2) \frac{d^2 \bar{E}(\eta)}{d\eta^2} . \quad (19)$$

The normalized parameters are defined by

$$n_e = \frac{q_e L_e k_L n_2}{\tau_a \beta_a \operatorname{Re}(\mathcal{L}_a) n_0} , \quad (20)$$

and

$$r = \frac{4\pi^2 c L_d}{\omega_L^3 T_a^2} \frac{d^2 n_0}{d\lambda^2} \quad (21)$$

[ $n = n_0 + n_2 |\bar{E}(\eta)|^2$ , is the nonlinear refractive index,  $L_{e,d}$  are the lengths of the nonlinear and of the dispersive media, and the factor  $q_e$  takes into account possible focusing or colliding pulse effects in the nonlinear media]. The effect of a small linear intensity loss  $\gamma$  (outcoupling mirror) can be introduced in a similar manner:

$$\delta_f \bar{E}(\eta) = -(\gamma/2) \bar{E}(\eta) . \quad (22)$$

As already mentioned, the relative position of each element in Fig. 1 is of no importance, because the corresponding transfer operators are expanded only to first-order terms. Accordingly, the total modification experienced in a complete round trip is the sum of the  $\delta_i \bar{E}$ . Thus we have

$$\bar{E}'(\eta + h) = \bar{E}(\eta) + \sum_{i=a,b,c,d,e,f} \delta_i \bar{E}(\eta) . \quad (23a)$$

By means of (23a) the temporal development of the pulse starting from spontaneous emission can be studied as well as the changes of the pulse parameters from round trip to round trip.

For certain values of the laser parameters steady-state solutions exist, which are characterized by

$$\sum_{i=a,b,c,d,e,f} \delta_i \bar{E} = 0 . \quad (23b)$$

For details concerning the numerical treatment of (23) we refer to Ref. 19.

Figure 6 presents the steady-state pulse parameters as functions of the Kerr-type nonlinearity and the dispersion. The presence of the photoisomer provides laser frequencies lying on the red arm of the ground-form absorption band, as known from experiment.<sup>17</sup> In Fig. 6 we have chosen laser parameters which provide counterbal-

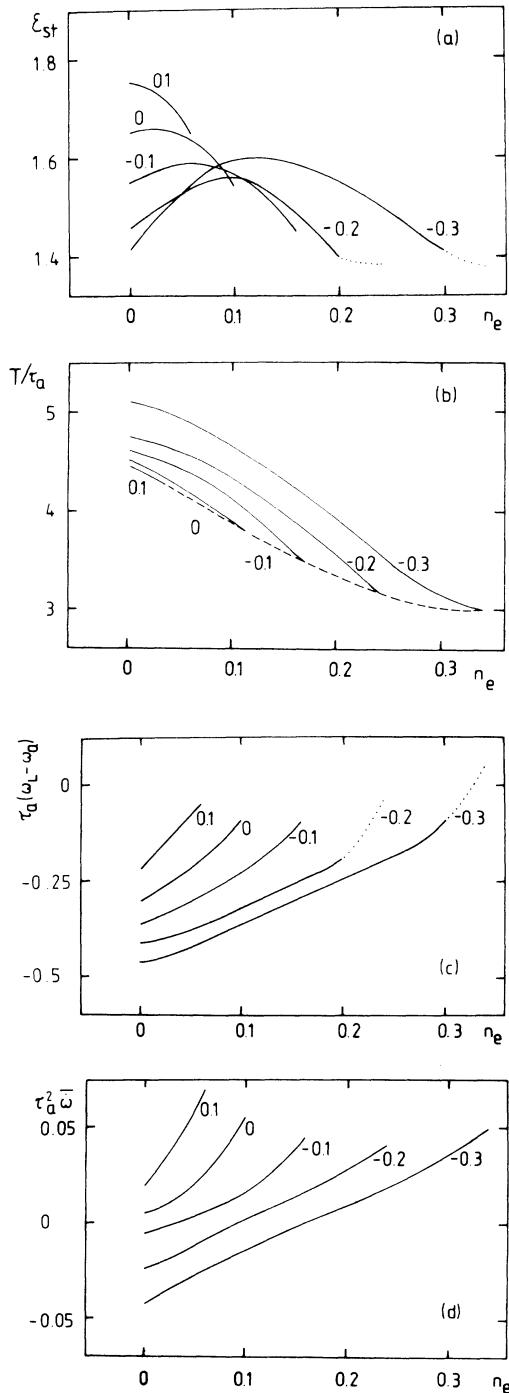


FIG. 6. Calculated steady-state pulse parameters vs non-linearity  $n_e$  and dispersion  $r$  (values indicated on the curves). (a) Steady-state pulse energy  $\epsilon_{st}$ , (b) normalized pulse duration  $T/\tau_a$ , (c) steady-state normalized relative frequency  $\tau_a(\omega_L - \omega_a)$ , (d) chirp parameter  $\tau_a^2 \bar{\omega}$ . Laser parameters:  $g_a = 0.3$ ,  $\kappa = 0.6$ ,  $U/T_a = 1$ ,  $\gamma = 0.05$ ,  $m_b^0 = 10$ ,  $m_c^0 = 7$ ,  $\tau_b/\tau_a = 3$ ,  $\tau_c/\tau_a = 2$ ,  $\tau_a(\omega_b - \omega_a) = 0$  and  $\tau_a(\omega_c - \omega_a) = -1$ . For modeling the photoisomerization we used  $W = 0.012$ ,  $\Phi_p = 0.04$  and  $\Phi_d = 0.08$ , according to Ref. 15. This results in variation of  $p$  in the range 3–3.2 in the figure. The boundary of the stable regime is indicated by a dashed line in (b).

ance of the chirping mechanisms in the absence of dispersion and nonlinearity. As can be seen, the mean chirp parameter

$$\tau_a^2 \bar{\omega} = \tau_a^2 \int_{-\infty}^{\infty} d\eta' \ddot{\phi}(\eta') |\bar{E}(\eta')|^2 / \int_{-\infty}^{\infty} d\eta' |\bar{E}(\eta')|^2 \quad (24)$$

is nearly equal to zero at  $r=0$  and  $n_e=0$ . Nevertheless, the quasiresonant media participate in the phase shaping when nonlinearity and dispersion are introduced. Keeping the nonlinearity at the constant zero value and adding negative dispersion results in chirping and simultaneous lengthening ( $\approx 10\%$ ) of the pulse duration. The chirping resembles, in this case, the pulse propagation in a dispersive medium, since the mean-chirp value at  $r = -0.3$ , for example, corresponds nearly to the value which, if compensated through extracavity propagation in a medium exhibiting opposite (positive) dispersion, would result in recompression of the pulse to its initial duration.

The combination of intracavity dispersion with nonlinearity of the opposite sign provides, however, an additional shortening mechanism. For increased values of  $r$ , the shortest pulses occur at maximum possible values of  $n_e$  just before instabilities set in. As can be seen from Fig. 6(b), the decrease of the pulse duration is saturated at large  $n_e$ . The shortest pulses are again slightly chirped, this time with the opposite sign (positive). The latter provides again the possibility of additional extracavity compression in a linear optical element exhibiting negative group velocity dispersion (GVD). Roughly, an overall achievable compression factor of about 2 can be estimated when increasing  $n_e$ .

Figure 6(c) shows that a change of the nonlinearity and, accordingly of the induced phase modulation, also results in a change of the mean-laser frequency. The latter is calculated imposing the condition that the first derivative of the slowly varying phase weighted by the pulse intensity vanishes.<sup>19</sup> This phase-modulation-induced frequency shift can be explained as follows. Due to the frequency change across the pulse and the different amplification and absorption of the leading pulse edge as compared with the trailing edge, the pulse spectrum can be shifted towards higher or lower frequencies after one round trip. In a limited parameter range only, this frequency shift can be compensated by the frequency dependence of the net gain, i.e., by the tendency to pull the pulse mid frequency to a position where the pulse experiences maximum net gain. This results in steady-state pulse parameters [23(b), cf. Fig. 6].

Outside this range, instabilities occur (dotted curves in Fig. 6) which are characterized by fluctuations of the pulse energy as well as of the pulse shape, duration, and phase modulation. Near the boundary of the stability range periodically (with the cavity round trip) oscillating laser parameters were found. This is shown in Fig. 7 for one set of laser parameters. The occurrence of such regimes are characterized by nonlinearities  $n_e$  exceeding a certain value and by too small a (negative) GVD.

In the extreme case, the induced frequency shift cannot be compensated and the laser is finally driven below threshold. If one increases the amplification here, the laser goes into a regime where both pulse edges experi-

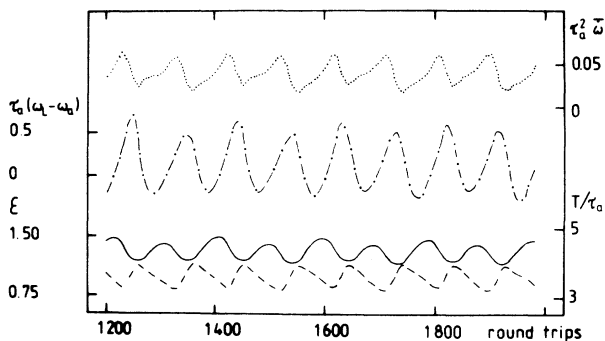


FIG. 7. Fluctuations of the laser parameters in a pulsing steady state achieved after 1200 round trips. The parameters are the same as in Fig. 6, and  $r = -0.2$  and  $n_e = 0.24$ . Pulse energy  $\varepsilon$  (solid line), normalized pulse duration  $T/\tau_a$  (dashed line), normalized relative laser frequency  $\tau_a(\omega_L - \omega_p)$  (dashed-dotted line), and integral chirp  $\tau_a^2 \bar{\omega}$  (dotted line).

ence net gain. The latter would lead to a continuous increase of the pulse duration and eventually to a breakup of the stable pulse regime. This behavior was not found in the absence of  $n_e$ ,<sup>19</sup> where an increase of the amplification (and pulse energy) always ensured a negative net gain at the trailing pulse edge due to high-gain saturation. It should also be noted that the instabilities begin to appear at energies  $\varepsilon_{st} \leq 1.4$ , cf. Fig. 6(a). With the parameters chosen in our example, at such energies, the gain depletion is not strong enough and the net gain behind the pulse edge becomes positive. The result is a broadening of the trailing edge and the occurrence of satellites which give rise to instabilities.

Under certain conditions, for too high an amplification coefficient, equally spaced multiple pulses can occur during one round-trip period. This, however, can be described by a decreased effective small signal gain for each pulse and is characterized by longer pulse durations. In this sense, the interplay of Kerr-type nonlinearity and linear dispersion represent the essential mechanism for the occurrence of instabilities in the passively mode-locked laser, which finally limit the achievable pulse duration.

Similar arguments as above are valid also for hybrid mode locking in the cases when the pulse durations are of the order of 100 fs and the intensities are relatively high, so that the dispersion and the Kerr-effect type nonlinearity have to be taken into account. Then, of course, the rate equation treatment of Sec. IV is not applicable. In the simulation of passive mode locking, the temporal pulse position is not bound to the pump pulse and a small shift  $h$  in the local time, which is constant in the steady state, is performed in each cavity round trip so that the pulse remains in the time interval considered. If this shift is assigned to a geometrical mismatch of the opposite sign, the results for passive mode locking can be interpreted also for the case of hybrid mode locking under optimum matching conditions. We note that the mean-pump intensities, i.e., averaged over the round trip time  $U$ , in both case are nearly the same. Neglecting in such a

way the effects of cavity mismatch, we can summarize that the main difference between passive and hybrid mode locking is that in the first case the intracavity pulse itself raises the amplification at the leading edge above the threshold, whereas in the second case the net amplification is already positive before the pulse arrives.

## VI. COMPARISON WITH EXPERIMENTS AND CONCLUSION

Only in the case of synchronous mode locking can single-shot streak camera measurements give direct information about the temporal shape of the (picosecond) pulses.<sup>23</sup> Fluctuations of the pulse parameters appear as bands in the low-frequency power spectrum of the laser, and therefore can be detected by an electronic spectrum analyzer.<sup>24</sup> The observed instabilities can be explained within the present model by the stochastic background introduced by spontaneous emission, which leads to severe distortions of the mode locking, especially for large intracavity filter bandwidth  $1/\tau_F$  and high pump energy. In this sense, spontaneous emission is the most limiting factor of the pulse duration in usual synchronously pumped lasers. Recent experiments<sup>25–28</sup> have shown that a reduction of the pump pulse width allows for the generation of shorter laser pulses and results in an improved laser stability. Since in the present model all quantities are normalized by the filter response time  $\tau_F$ , a shorter pump pulse corresponds to a smaller value of the numerical quantity  $T_p/\tau_F$ . Thus a shorter pump pulse is equivalent to a longer filter response time and both dependencies are included in the model. For small values of  $T_p/\tau_F$  ( $T_p/\tau_F < 100$ ), it is known<sup>8,28</sup> that the main limit of the laser pulse width is given by the pump pulse width and the filter bandwidth, respectively, and not by spontaneous emission. The only problem, with respect to the determination of the laser pulse width in dependence on pump pulse duration and filter bandwidth, consists in the invalidity of the REA approximation for pump pulses in the subpicosecond range. In this region the full system of Maxwell-Bloch equations should be solved.

By a similar method, as in Ref. 24 the instabilities in hybrid-mode-locked<sup>29</sup> and passively mode-locked<sup>30</sup> systems have been studied. The authors ascribe the large energy fluctuations in synchronous mode locking<sup>24</sup> to random pulse substructure, which, neglecting the jitter arising from the pump laser, supports the statement of Ref. 9 that only a quasi-steady-state can be achieved in these lasers. Our analysis supports the latter, in that spontaneous emission is the stochastic background for the occurring disturbances. Studies of the hybrid-mode-locked system revealed only several percent energy fluctuations and up to 50% pulse duration fluctuations for 250 fs pulses,<sup>29</sup> together with a much longer time necessary for the establishment of a steady-state.

The passively mode-locked laser exhibited  $\approx 15\%$  fluctuations of the pulse duration for 50 fs pulses and energy fluctuations as high as 80% on the boundary of the stability region. These were identified as such arising from the phase-shaping mechanisms. Our model explains them at



the extreme short pulse duration and high pulse intensity by the influence of the Kerr effect. The linear dispersion alone is compatible with the other pulse shaping mechanisms, such as saturable absorption and gain. This is supported by the nearly symmetric dispersion dependence of the pulse duration for longer pulses, as discussed in Ref. 19 and experimentally measured in Ref. 11, as well as in Ref. 31, at low intracavity pulse energies. At larger nonlinearities the pulse duration decreases with increasing net GVD and reaches its minimum just at the boundary of the stability range. This behavior is also in qualitative agreement with experiments.<sup>17</sup> For this reason, the control of higher-order dispersion terms in the presence of the Kerr effect seems to be useful to achieving even short-pulse durations.

Our results can offer certain explanations for the observation of pulses which are not bandwidth limited. In Ref. 18 the 73 fs pulses were shortened to 50 fs by addition of highly nonlinear solvent in the absorber solution and after optimizing the dispersion. This shortening was accompanied by a much larger spectral broadening from 9.1 to 14.1 nm, which gives a (pulsewidth) × (bandwidth) product of 0.6. According to our model, this result could be assigned to a fluctuating pulse duration and to a fluctuating mean frequency. Also, the shift to shorter wavelengths reported when increasing the nonlinearity is in agreement with our results.

The onset of instabilities at certain values of the nonlinearity and GVD leads to periodic oscillations of the pulse parameters, including energy and spectrum, and is in agreement with experimental observations.<sup>11,32</sup> These

experimental findings<sup>11,32,33</sup> were ascribed to solitonlike pulse propagation. Such solitonlike behavior of the pulses in femtosecond dye lasers was suggested for the first time in Refs. 6 and 34. Some of the experimental data were tried to be explained by the so-called nonlinear Schrödinger equation (NLSE) alone, which describes pulse propagation in a medium with (group velocity) dispersion and (Kerr-type) nonlinearity. In this manner, the essential influence of saturable absorption and gain for passive mode locking is neglected. As opposed, our model of passive mode locking can also be regarded as the treatment of the NLSE modified by a nonlinear polarization arising from the active media and is equivalent to the search for stable pulse solutions. Thus our calculations explain the energy fluctuations, the asymmetrical spectral shapes, and the shift of the whole spectrum over nearly one half width<sup>33</sup> by the interplay of dispersion, nonlinearity, and frequency dependent saturable absorption and gain.

Limits of our model in describing passively mode-locked lasers rest mainly on the description of the active media as homogeneously broadened two-level systems, which represent the simplest model to account for saturable absorption, depletable, gain, and phase memory. In principle, at the expense of computer time, the model used can also deal with inhomogeneously broadened transitions. The latter seems to play a part in the interaction of ultimate short pulses with organic dyes.<sup>35</sup> From detailed studies of the pulse chirping in homogeneous broadened media<sup>36</sup> we expect, however, that the main processes discussed above remain valid.

- 
- <sup>1</sup>J. Herrmann and B. Wilhelmi, *Lasers for Ultrashort Light Pulses* (Elsevier, Amsterdam, 1987).
- <sup>2</sup>J. A. Valdmanis, R. L. Fork, and J. P. Gordon, *Opt. Lett.* **10**, 131 (1985).
- <sup>3</sup>H. Kubota, K. Kurokawa and M. Nakazawa, *Opt. Lett.* **73**, 749 (1988).
- <sup>4</sup>J. Herrmann and U. Motschmann, *Appl. Phys. B* **27**, 27 (1982).
- <sup>5</sup>J. Herrmann and F. Weidner, *Appl. Phys. B* **27**, 105 (1982).
- <sup>6</sup>W. Rudolph and B. Wilhelmi, *Appl. Phys. B* **35**, 37 (1984).
- <sup>7</sup>J. Herrmann and U. Motschmann, *Opt. Commun.* **40**, 379 (1982).
- <sup>8</sup>D. Schubert, U. Stamm, and B. Wilhelmi, *Opt. Quant. Elect.* **17**, 337 (1985).
- <sup>9</sup>J. M. Catherall and G. H. C. New, *IEEE J. Quantum. Electron.* **QE-22**, 1593 (1986).
- <sup>10</sup>V. Petrov, W. Rudolph, and B. Wilhelmi, *Opt. Quant. Elect.* **19**, 377 (1987).
- <sup>11</sup>H. Avramopoulos, P. M. W. French, J. A. R. Williams, G. H. C. New, and J. R. Taylor, *IEEE J. Quantum. Electron.* **QE-24**, 1884 (1988).
- <sup>12</sup>U. Stamm, *Appl. Phys. B* **45**, 101 (1988); U. Stamm, and F. Weidner, *Opt. Commun.* **63**, 179 (1987).
- <sup>13</sup>R. S. Putnam, *J. Opt. Soc. Am. B* **1**, 771 (1984).
- <sup>14</sup>J. M. Catherall, G. H. C. New, and P. M. Radmore, *Opt. Lett.* **7**, 319 (1982).
- <sup>15</sup>L. M. Frantz and J. S. Nodvik, *J. Appl. Phys.* **34**, 2346 (1963).
- <sup>16</sup>S. Rentsch, E. Döpel, and V. Petrov, *Appl. Phys. B* **46**, 354 (1988).
- <sup>17</sup>J.-C. Diels, W. Dietel, J. J. Fontaine, W. Rudolph, and B. Wilhelmi, *J. Opt. Soc. Am. B* **2**, 680 (1986); J. A. Valdmanis and R. L. Fork, *IEEE J. Quantum. Electron.* **QE-22**, 112 (1986).
- <sup>18</sup>M. Yamashita, K. Torizuka, and T. Sato, *Opt. Lett.* **13**, 24 (1988).
- <sup>19</sup>V. Petrov, W. Rudolph, and B. Wilhelmi, *Rev. Phys. Appl.* **22**, 1639 (1987).
- <sup>20</sup>H. A. Haus, *IEEE J. Quantum. Electron.* **QE-11**, 736 (1975).
- <sup>21</sup>G. H. C. New, *IEEE J. Quantum. Electron.* **QE-10**, 115 (1974).
- <sup>22</sup>B. Wilhelmi, W. Rudolph, E. Döpel, and W. Dietel, *Opt. Acta.* **32**, 1175 (1985).
- <sup>23</sup>K. Smith, J. M. Catherall, G. H. C. New, *Opt. Commun.* **58**, 118 (1986).
- <sup>24</sup>D. von der Linde, *Appl. Phys. B* **39**, 201 (1986).
- <sup>25</sup>B. Beaud and B. Zysset, *Opt. Lett.* **11**, 24 (1986).
- <sup>26</sup>A. M. Johnson and W. M. Simpson, *J. Opt. Soc. Am. B* **2**, 619 (1985).
- <sup>27</sup>G. Angel, R. Gagel, and A. Laubereau, *Opt. Commun.* **63**, 259 (1987).
- <sup>28</sup>Sh. Burdulis, R. Grigonis, T. Damm, A. Piskarskas, G. Sinkavicius, V. Sirutkaitis, U. Stamm, and K. Vogler, in *European Conference on Quantum Electronics, Hanover, 1988* (unpublished).
- <sup>29</sup>D. Kühlke, U. Herpers, and D. von der Linde, *Appl. Phys. B* **38**, 233 (1985).
- <sup>30</sup>D. Kühlke, T. Bonkhofer, and D. von der Linde, *Opt. Commun.* **59**, 208 (1986).
- <sup>31</sup>J. C. Diels, W. Dietel, and J. J. Fontaine, *Opt. Lett.* **8**, 4 (1983).

- <sup>32</sup>F. W. Wise, I. A. Walmsley, and C. L. Tang, *Opt. Lett.* **13**, 129 (1988).
- <sup>33</sup>F. Salin, P. Graingier, G. Roger, and A. Brun, *Phys. Rev. Lett.* **56**, 1132 (1986); **60**, 569 (1988).
- <sup>34</sup>O. E. Martinez, R. L. Fork, and J. P. Gordon, *J. Opt. Soc. Am. B* **2**, 753 (1985).
- <sup>35</sup>C. H. BritoCruz, R. L. Fork, W. H. Knox, and C. V. Shank, *Chem. Phys. Lett.* **132**, 341 (1986).
- <sup>36</sup>V. Petrov, W. Rudolph, and B. Wilhelmi (unpublished).